



## Article

# Redox-neutral photocatalytic strategy for selective C–C bond cleavage of lignin and lignin models via PCET process

Yinling Wang, Yue Liu, Jianghua He<sup>\*</sup>, Yuetao Zhang<sup>\*</sup>

State Key Laboratory of Supramolecular Structure and Materials, College of Chemistry, Jilin University, Changchun 130012, China

## ARTICLE INFO

## Article history:

Received 31 August 2019

Received in revised form 2 September 2019

Accepted 2 September 2019

Available online 9 September 2019

## Keywords:

C–C bond cleavage

Lignin depolymerization

Photocatalysis

Proton-coupled electron transfer

Redox-neutral

## ABSTRACT

It remains challenging to achieve the selective cleavage of C–C bonds in lignin or lignin model compounds to produce aromatic products in high yield and selectivity. We have developed a redox-neutral photocatalytic strategy to accomplish this goal in both  $\beta$ -O-4 and  $\beta$ -1 lignin models at room temperature (RT) via proton-coupled electron transfer (PCET) process without any pretreatments of substrate, by adjusting the alkalinity of base to obtain a lignin models/base PCET pair with a bond dissociation free energy close to 102 kcal/mol. Without breaking down  $C_{\beta}$ – $C_{\gamma}$  bond and any C–O bonds, this PCET method is 100% atom economy and produces exclusive  $C_{\alpha}$ – $C_{\beta}$  bond cleavage products, such as benzaldehydes (up to 97%) and phenyl ethers (up to 96%), in high to excellent yields and selectivities. Preliminary studies indicated that the PCET strategy is also effective for the depolymerization of native lignin at RT, thus providing significantly important foundation to the depolymerization of lignin.

© 2019 Science China Press. Published by Elsevier B.V. and Science China Press. All rights reserved.

## 1. Introduction

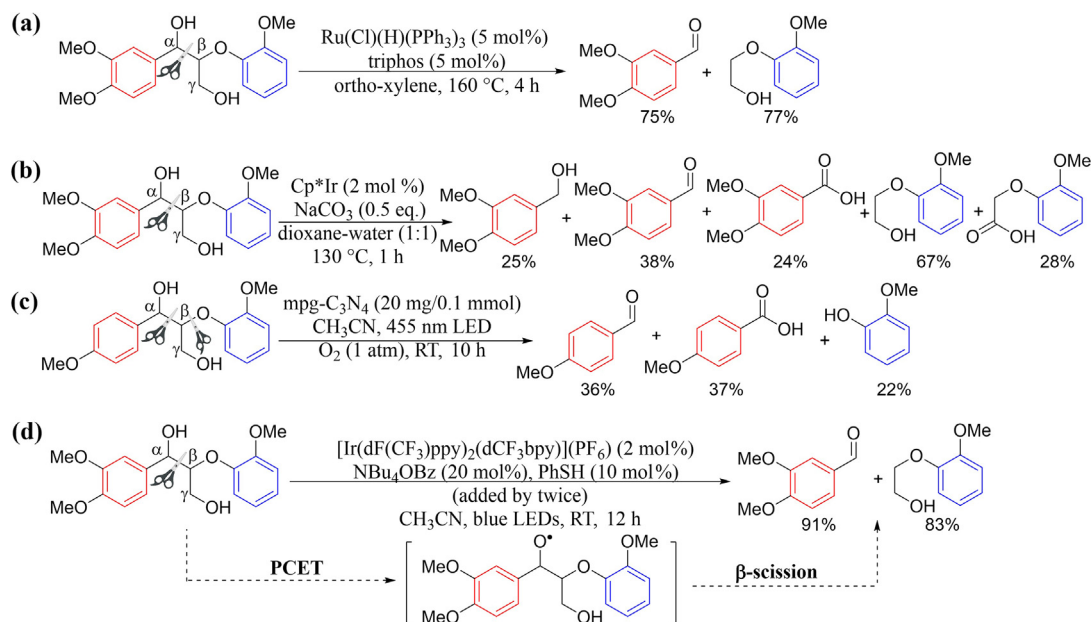
As a heterogeneous aromatic biopolymer accounting for nearly 30% of non-fossil organic carbon [1] as well as the only natural resource of aromatic chemicals on the earth [2], lignin depolymerization could provide renewable alternatives to the depleted fossil resources for production of aromatics. However, only less than 5% of lignin is used to deliver commercial products [2–4], because of its complicated polymeric structure and inherent inert chemical activities [5]. Various methods have been developed for effective cleavage of C–O bonds in both lignin and lignin model compounds [6–14]. In comparison with the comprehensive studies of C–O bond cleavage, only a handful of examples were reported for selective C–C bond cleavage in lignin or lignin model compounds due to its higher dissociation energies [15–17] than that of C–O bond. Such as in 2015, Klankermayer group [18] reported a selective redox-neutral cleavage of  $C_{\alpha}$ – $C_{\beta}$  in  $\beta$ -O-4 lignin models catalyzed by ruthenium-triphos complexes at 160 °C (Scheme 1a). Activation of the primary alcohol by  $Cp^*Ir$ -bpyridonate catalyst enabled the  $C_{\alpha}$ – $C_{\beta}$  bond cleavage of lignin at 130 °C, affording a range of non-phenolic monomers (Scheme 1b) [19]. Recently, some advancements have been achieved in the application of photochemical strategy to the depolymerization of lignin under mild conditions [9,20–25]. Wang and

co-workers [24] reported a photocatalytic oxidative strategy for C–C bond cleavage along with  $C_{\beta}$ –O bond cleavage in lignin  $\beta$ -O-4 linkages using a mesoporous graphitic carbon nitride catalyst (mpg- $C_3N_4$ ), furnishing 4-methoxybenzaldehyde, 4-methoxybenzoic acid and 2-methoxyphenol in 36%, 37% and 22% yield, respectively (Scheme 1c). From the above overview, there are still some challenges to be solved in the selective cleavage of C–C bonds of lignin and lignin model compounds, such as harsh reaction conditions [18,19], inefficient C–C bond cleavage, low product yield and selectivity as well as being accompanied with the cleavage of C–O bonds or loss of  $\gamma$ - $CH_2OH$  sometimes [24,26–29]. Therefore, it is a great impetus for researchers to develop new strategy to solve these problems.

As the most dominant linkage in both softwood and hardwood,  $\beta$ -O-4 linkages accounts for around 50% of all linkages found in lignin [3,4], represented by a secondary benzylic hydroxyl group at the  $C_{\alpha}$  position and a primary hydroxyl group at  $C_{\gamma}$  position [30]. Oxidation of  $\alpha$ -OH into ketone structure with a lower dissociation energy of C–O bond has been demonstrated to be an effective strategy for lignin depolymerization [30–34]. Recently, we successfully applied the classic organic named reaction to the selective cleavage of C–C bonds in oxidized  $\beta$ -O-4 lignin models and produced various useful platform chemicals in high to excellent yields, such as multifunctional esters through Baeyer-Villiger oxidation [28] and N-substituted aromatics via Beckmann rearrangement [29]. However, instead of pretreating  $\alpha$ -OH or  $\gamma$ -OH at the expense of extra energy cost and multi-steps, it would be more desirable to develop a depolymerization strategy with better atom economy for

<sup>\*</sup> Corresponding authors.

E-mail addresses: [hjh2015@jlu.edu.cn](mailto:hjh2015@jlu.edu.cn) (J. He), [ytzhang2009@jlu.edu.cn](mailto:ytzhang2009@jlu.edu.cn) (Y. Zhang).



**Scheme 1.** (Color online) C<sub>α</sub>-C<sub>β</sub> bond cleavage in β-O-4 lignin models. (a) Previous work: Ru-catalyzed selective C<sub>α</sub>-C<sub>β</sub> bond cleavage [18]; (b) Previous work: Ir-catalyzed selective C<sub>α</sub>-C<sub>β</sub> bond cleavage [19]; (c) Previous work: visible-light-driven mpg-C<sub>3</sub>N<sub>4</sub>-catalyzed C<sub>α</sub>-C<sub>β</sub> bond cleavage [24]; (d) This work: visible-light-driven Ir-catalyzed selective C<sub>α</sub>-C<sub>β</sub> bond cleavage.

selective C-C bond cleavage by taking full advantage of these α-OH groups of lignin rather than pretreating or protecting them.

Proton-coupled electron transfer (PCET) is referred to a reaction where a proton and electron are transferred in a single, concerted step and found in numerous important biological redox processes and organic technologies for activation of small molecule as well [35–41]. Knowles and co-workers [42] discovered that the alkoxy radical, formed from the photocatalytic homolytic activation of benzylic hydroxyl group via a PCET process, could weaken the adjacent C-C bonds to enable the β-scission, thus realizing the ring-opening of cyclic alcohol. Considering structural similarity between the benzylic hydroxyl group and α-OH group in β-O-4 linkages as well as the high reactivity of photocatalytic characteristics under mild conditions [43–46], we envisioned that PCET strategy might enable us to overcome the above-mentioned barriers in C-C bond cleavage and achieve the desired products from depolymerization of lignin model compounds and lignin without pretreatment. Here we utilized an Ir-containing catalyst to achieve a one-step, visible-light-driven photocatalytic depolymerization of lignin model compounds through PCET process at RT. To the best of our knowledge, it is the first time that PCET photocatalytic strategy successfully solved the above-mentioned problems without pretreating lignin models [47], not only achieving high selectivity in the cleavage of C<sub>α</sub>-C<sub>β</sub> bond without the breakdown of any C-O bonds, but also furnishing C<sub>α</sub>-C<sub>β</sub> bond cleavage products in high to excellent yields and selectivities, thus giving rise to a 100% atom-economy. More importantly, this PCET method enabled us to achieve the first example of redox-neutral, photocatalytic depolymerization of real lignin at RT.

## 2. Experimental

### 2.1. General information

All syntheses and manipulations of air- and moisture-sensitive materials were carried out in flamed Schlenk-type glassware on a

dual-manifold Schlenk line, a high-vacuum line, or an argon-filled glovebox.

Phenol, diisopropylamine, 2-bromoacetophenone, 2-bromo-4'-methoxyacetophenone, 2-bromo-1-(3-methoxyphenyl)ethenone, sodium borohydride, ethyl (2-methoxyphenoxy)acetate, KF, iridium trichloride, inorganic salts, solvents, and the standard substances benzaldehyde, *p*-methoxybenzaldehyde, *m*-methoxybenzaldehyde, 2,4-dimethoxybenzaldehyde, anisole, *o*-methoxyanisole, *m*-methoxyanisole, *o*-methylanisole, 2-phenoxyethanol, and toluene were purchased from Adamas-beta®. Benzylmagnesium chloride, *n*-BuLi (1.6 mol/L solution in hexanes), guaiacol, 2-chloro-5-(trifluoromethyl)pyridine, 2-MeO-pyridine, 4-MeO-pyridine, 2,4-difluorophenylboronic acid, tri(dibenzylideneacetone)dipalladium, and DMAP were purchased from J&K. Tetrakis(triphenylphosphine) palladium, AgPF<sub>6</sub>, bipyridine, and collidine were purchased from Energy. Thiophenol was purchased from Xiya. All of chemicals were used as received unless otherwise specified as follows. THF were dried over sodium/potassium alloy distilled under nitrogen atmosphere prior to use for the synthesis of lignin model compound. CH<sub>3</sub>CN were dried over CaH<sub>2</sub> distilled under nitrogen atmosphere prior to use for light-induced catalytic reactions. Thiophenol were dried over 4 Å molecular sieve. Please check [Supporting materials](#) (online) for the synthesis of lignin model compounds and Ir-containing catalysts.

Reactions were monitored by thin layer chromatography (TLC) visualizing with ultraviolet light (UV). Column chromatography purifications were carried out using silica gel. The reaction mixture was analyzed using Waters high performance liquid chromatograph (HPLC) system equipped with autosampler, C18 column (length: 75 mm, internal diameter: 4.6 mm, 35 °C) and UV/Vis detector (λ = 220 nm). CH<sub>3</sub>OH:H<sub>2</sub>O (40:60) was used as a mobile phase with a flow rate of 1.0 mL/min. NMR spectra were recorded on a Bruker Avance II 500 (500 MHz, <sup>1</sup>H; 126 MHz, <sup>13</sup>C) instrument at room temperature (RT). Chemical shifts for <sup>1</sup>H and <sup>13</sup>C spectra were referenced to internal solvent resonances. Mass spectra were recorded on the Bruker MicroTOF Q II. The GC-MS were recorded on a Trace Ultra DSQ. GC analysis information: Agilent Technologies 6890 equipped with an Agilent US0769531J

(DBWAX 15 m  $\times$  0.320 mm  $\times$  0.25  $\mu$ m) capillary column and a flame ionization detector; carrier gas: N<sub>2</sub> (2 mL/min); temperature program: 60 °C (1 min); 5 °C/min to 210 °C (7 min); 5 °C/min to 220 °C (5 min); injector temperature: 250 °C; detector temperature: 250 °C; split ratio: 30; injection volume: 5  $\mu$ L. Yield were determined by GC analysis using naphthalene as internal standard. Lignin number-average molecular weight ( $M_n$ ) and molecular weight distributions ( $PDI = M_w/M_n$ ) were measured by gel permeation chromatography (GPC) at 40 °C and a flow rate of 1 mL/min, with THF (HPLC grade) as an eluent on a Waters 1515 instrument equipped with Waters 4.6  $\times$  30 mm guard column and three Waters WAT054466, WAT044226, WAT044223 columns. The instrument was calibrated with PS standards, and chromatograms were processed with Waters Breeze2 software.

## 2.2. General procedure for PCET reaction using lignin models as substrate

### 2.2.1. Using lignin model **A–K** or **P** as substrate

A 10 mL Schlenk tube was charged with lignin model compound such as **A–K** or **P** (0.1 mmol, 1.0 eq.), **Ir-1** (2 mol%), redistilled collidine (20 mol%), redistilled PhSH (10 mol%) and 2 mL anhydrous CH<sub>2</sub>Cl<sub>2</sub> under N<sub>2</sub> atmosphere. The reaction was irradiated by blue LED lamp (50 W/100 W) at RT for 12 h. The resulting mixture was dissolved to constant volume in a 50 mL volumetric flask and then filtered. The filtrate was measured by HPLC.

### 2.2.2. Using lignin model **L–O** as substrate

A 10 mL Schlenk tube was charged with lignin model compound such as **L–O** (0.1 mmol, 1.0 eq.), **Ir-1** (1 mol%), NBu<sub>4</sub>OBz (10 mol%), redistilled PhSH (5 mol%) and 2 mL anhydrous CH<sub>3</sub>CN under N<sub>2</sub> atmosphere. The reaction was irradiated by blue LED lamp (100 W) at RT for 6 h. Then **Ir-1** (1 mol%), NBu<sub>4</sub>OBz (10 mol%), redistilled PhSH (5 mol%) were added under N<sub>2</sub> atmosphere and irradiated by blue LED lamp (100 W) at RT for another 6 h. The resulting mixture was dissolved to constant volume in a 50 mL volumetric flask and then filtered. The filtrate was measured by HPLC.

## 2.3. Extraction and depolymerization of lignin

### 2.3.1. Extraction of birch-dioxane-lignin (**BDL**)

10.0 g birch saw dust, 50 mL 1,4-dioxane and 1.7 mL HCl (37 wt%) were introduced in a round bottom flask. The flask was put in an oil bath and heated at 85 °C for 3 h under reflux. After cooling down to room temperature, 3.36 g NaHCO<sub>3</sub> was added to the mixture and stirred for another 30 min. The reaction mixture was then filtered and washed with 10 mL of dioxane. The resulting solution was then concentrated at 40 °C under reduced pressure. The resulting dark brown oil was diluted with 30 mL EtOAc and then added dropwise to 500 mL of hexane to precipitate the lignin. After filtration, the collected lignin was washed with hexane (50 mL) followed by diethyl ether (50 mL) for 5 min each while sonicating. The recovered lignin was then dried overnight at room temperature in a desiccator to afford 1.36 g **BDL**.

### 2.3.2. Preparation of birch-dioxane-MeI-lignin (**BDIL**)

**BDL** (150 mg) was dissolved in DMF 10 mL, K<sub>2</sub>CO<sub>3</sub> (207 mg) was added. And then methyl iodide (213 mg) was added dropwise, and reacted at room temperature for 24 h. The mixture was diluted with water 50 mL and extracted with dichloromethane (2  $\times$  20 mL). The organic layer was dried over Na<sub>2</sub>SO<sub>4</sub> and concentrated to  $\sim$ 2 mL under reduced pressure. To precipitate the lignin, this solution was added dropwise to 100 mL of hexane that was being stirred. After filtration, the collected lignin was then washed with hexane (50 mL) followed by diethyl ether (50 mL) for 5 min

each while sonicating. The recovered lignin was then dried overnight at room temperature in a desiccator to afford 94 mg birch-dioxane-MeI-lignin (**BDIL**).

### 2.3.3. Depolymerization of lignin

Under nitrogen conditions, 20 mg of lignin, 1.1 mg of **Ir-1**, 3.6 mg NBu<sub>4</sub>OBz and 0.5  $\mu$ L PhSH were dissolved in 2.0 mL dry CH<sub>3</sub>CN within a 10 mL Schlenk bottle. The reactor was excited for 12 h under a 100 W blue light at room temperature. And then under nitrogen conditions, the second batch of 1.1 mg of **Ir-1**, 3.6 mg NBu<sub>4</sub>OBz and 0.5  $\mu$ L PhSH was added and illuminated for another 12 h. After the reaction, the resulting mixture was dissolved to constant volume in a 10 mL volumetric flask, naphthalene as internal standard, and then filtered with a PTFE syringe filter and quantified by GC-FID, GPC and <sup>1</sup>H NMR.

## 3. Results and discussion

### 3.1. Optimization of the reaction conditions

Due to its efficient luminescence and visible-light absorption [48], Ir-containing complexes have been utilized in the application of electroluminescence devices [49], photocatalytic reactions [50,51], solar cells [52], as well as in the activation of O–H or N–H bonds via PCET process [35–42]. It is generally recognized that PCET process possessed lower energy than that carried by reactions went through stepwise electron-transfer or proton-transfer pathways, therefore, it is relatively faster [35–37]. Its corresponding ability to transfer proton (H<sup>+</sup>) together with electron (e<sup>−</sup>) could be defined by bond dissociation free energy (BDFE (kcal/mol) = 23.06  $E$  + 1.37 pK<sub>a</sub> + 54.9 (RT in MeCN)) of the oxidant/base pair [35–42]. Herein, pK<sub>a</sub> represents the alkalinity of base [38–41,53], whereas  $E$  is referred to the half-wave reduction potential ( $E_{p/2}$ ) of lignin model serving as an internal oxidant, could be measured by cyclic voltammetry. As previously reported by Knowles et al. [42,54], the PCET activation of O–H bond followed by  $\beta$ -scission of C–C bond is enabled only if the “BDFE” of the corresponding oxidant/base PCET pair is close to the bond dissociation energy (BDE) of O–H bond (102 kcal/mol). According to the definition of BDFE, both the alkalinity of base and the redox potential of oxidant play significantly important role in affecting the PCET reactivity.

After fixing 1-(4-methoxyphenyl)-2-phenoxyethan-1-ol (**A**,  $E_{p/2}$  = 1.16 V vs. Fc/Fc<sup>+</sup>) as model substrate, PhSH as H-atom donor and [Ir(dF(CF<sub>3</sub>)ppy)<sub>2</sub>(5,5'-d(CF<sub>3</sub>)bpy)](PF<sub>6</sub>) (**Ir-1**,  $E_{1/2}$  = 1.3 V vs. Fc/Fc<sup>+</sup>) (Fig. 1) as catalyst, we examined the effectiveness of five different bases for C–C bond cleavage via PCET process under 50 W blue LED irradiation at RT for 12 h. The combination of 2-MeO-pyridine (pK<sub>a</sub> = 9.9) with model **A** had a BDFE value of 95 kcal/mol, which is lower than the BDE of O–H bond (102 kcal/mol), thus being ineffective for C $\alpha$ –C $\beta$  bond cleavage (Table 1, entry 1). Using more basic NBu<sub>4</sub>OP(O)(OBu)<sub>2</sub> (pK<sub>a</sub> = 13) furnished an enhanced BDFE value of 99 kcal/mol, thus producing corresponding C $\alpha$ –C $\beta$  bond cleavage product, *p*-anisaldehyde (**aa**) in 50% yield and anisole (**ba**) in 51% yield, respectively (Table 1, entry 2). The employment of collidine (pK<sub>a</sub> = 14.98) with even higher alkalinity enabled us to obtain a BDFE value of 101 kcal/mol. To our gratification, this model **A**/collidine PCET pair not only exhibited excellent selectivity in the cleavage of C $\alpha$ –C $\beta$  bond without the breakdown of C $\beta$ –O bond, but also afforded corresponding C $\alpha$ –C $\beta$  bond cleavage products **aa** and **ba** in 94% and 93% yield, respectively (Table 1, entry 3). Excellent isolated yield (93% **aa**; 91% **ba**, Scheme S1 online) could be achieved by the gram-scale reaction using lignin model **A** as substrate. Using DMAP (pK<sub>a</sub> = 18) and NBu<sub>4</sub>OBz (pK<sub>a</sub> = 21.5) with even higher alkalinity than that of collidine afforded the further enhanced BDFE value

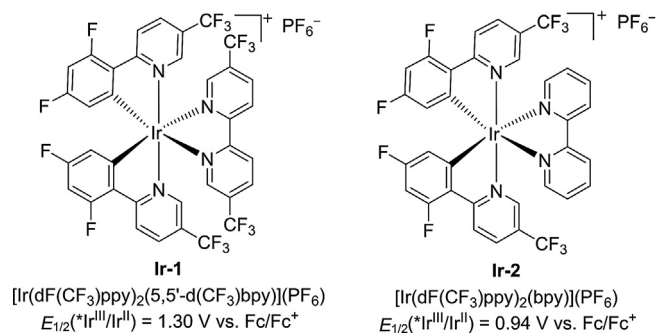


Fig. 1. The structure of Ir-containing catalysts.

Table 1

Investigation of the photocatalytic  $\text{C}_\alpha\text{-C}_\beta$  bond cleavage in lignin model **A** via PCET process.<sup>a</sup>

Entry	Base	BDFE <sup>b</sup>	Yield (%) <sup>c</sup>	
			aa	ba
1	2-MeO-pyridine ( $\text{pK}_a = 9.9$ )	95	<1	<1
2	$\text{NBu}_4\text{OP}(\text{O})(\text{OBu})_2$ ( $\text{pK}_a = 13$ )	99	50	51
3	Collidine ( $\text{pK}_a = 14.98$ )	102	94	93
4	DMAP ( $\text{pK}_a = 18$ )	106	<1	<1
5	$\text{NBu}_4\text{OBz}$ ( $\text{pK}_a = 21.5$ )	111	6	4
Entry	Change from standard condition (Entry 3)		aa	ba
6	No light		0	0
7	No photocatalyst		0	0
8	No base		0	0
9	No PhSH		5	7
10	$\text{H}_2\text{O}$ (1.0 eq.)		85	86
11	$\text{O}_2$ atmosphere		0	0
12	<b>Ir-2</b>		3	5

<sup>a</sup> Reaction was illuminated with 50 W blue LED irradiation in  $\text{N}_2$  atmosphere at RT for 12 h, with 0.1 mmol substrate, 2 mol% **Ir-1**, 20 mol% collidine, 10 mol% PhSH, 2 mL  $\text{CH}_2\text{Cl}_2$ .

<sup>b</sup> BDFE (kcal/mol) =  $23.06 E_{\text{p}/2} + 1.37 \text{ pK}_a + 54.9$  (RT in MeCN).

<sup>c</sup> The yields were measured by HPLC.

of 106 and 111 kcal/mol, respectively. However, both of them only produced negligible amounts of **aa** and **ba** (Table 1, entries 4 and 5), probably resulting from the incapability of PCET pair due to the incompatibility between lignin model substrate and relatively strong base [37].

With the identification of efficient model **A**/collidine PCET pair, we started to examine effects of different reaction parameters on reaction. It turned out that light, photocatalyst, base, and PhSH are essentially important to this PCET reaction. It would be completely shut down in the absence of any of light, photocatalyst and base (Table 1, entries 6–8) or only yielded trace amounts of products without PhSH (Table 1, entry 9). It should be noted that adding one equiv of water to reaction still produced **aa** and **ba** in 85% and 86% yield (Table 1, entry 10), respectively, indicating that the PCET process is not highly sensitive to moisture. However, oxygen is extremely detrimental to PCET reaction, thus completely shutting down reaction (Table 1, entry 11). Different Ir-containing catalysts were also examined for this reaction. It turned out that the employment of  $[\text{Ir}(\text{dF}(\text{CF}_3)\text{ppy})_2(\text{bpy})](\text{PF}_6)$  (**Ir-2**) (Fig. 1), with a redox potential ( $E_{1/2} = 0.94 \text{ V vs. Fc/Fc}^+$ ) lower than that of model **A** ( $E_{\text{p}/2} = 1.16 \text{ V vs. Fc/Fc}^+$ ), led to a drastically decreased yield of **aa** (3%) and **ba** (5%), respectively (Table 1, entry

12). This result revealed that a catalyst must have a redox potential higher than that of lignin model to enable the PCET reaction.

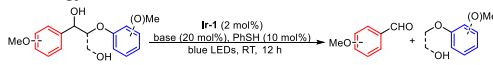
### 3.2. Substrate scope

With the optimized conditions in hand, we further expanded substrate scope. PCET pair containing lignin model **B** ( $E_{\text{p}/2} = 1.21 \text{ V vs. Fc/Fc}^+$ , BDFE = 103 kcal/mol) exhibited high selectivity and produced benzaldehyde (**ab**) in 95% yield and **ba** in 93% yield, respectively (Table 2, entry 2). It is noted that the PCET reaction could tolerate fluoride at para-position of phenyl ring (left, red), such as 1-(4-fluorophenyl)-2-phenoxyethan-1-ol (**C**), achieving 4-fluorobenzaldehyde (**ac**) in 92% yield and **ba** in 91% yield, respectively (Table 2, entry 3). With methoxyl at metha-position of phenyl ring (left, red), 1-(3-methoxyphenyl)-2-phenoxyethan-1-ol (**D**) produced 3-methoxybenzaldehyde (**ad**) in 95% yield and **ba** in 92% yield, respectively (Table 2, entry 4). Comparable results were also achieved by 1-(4-methoxyphenyl)-2-(*o*-tolylloxy)ethan-1-ol (**E**, 95% yield of **aa** and 96% yield of 1-methoxy-2-methylbenzene (**bb**)) with methyl group at ortho-position of phenoxy (right, blue) and 2-(3-methoxyphenoxy)-1-(4-methoxyphenyl)ethan-1-ol (**F**, 94% yield of **aa** and 93% yield of 1,3-dimethoxybenzene (**bc**)) with methoxy group at metha-position of phenoxy (right, blue) (Table 2, entries 5 and 6). Using 2-(2-methoxyphenoxy)-1-(4-methoxyphenyl)ethan-1-ol with a methoxy group at ortho-position of phenoxy (right, blue) (**G**) as substrate led to the production of **aa** and 1,2-dimethoxybenzene (**bd**) in 89% and 86% yield, respectively (Table 2, entry 7). This strategy is also effective for reaction using lignin model compounds with  $\gamma\text{-OH}$  as substrate, achieving good to excellent product yield (80% yield of **ab** and 78% yield of **be** for 2-phenoxy-1-phenylpropane-1,3-diol (**H**); 97% yield of **aa** and 90% yield of 2-phenoxyethan-1-ol (**be**) for 1-(4-methoxyphenyl)-2-phenoxypropane-1,3-diol (**I**); 94% yield of **aa** and 91% yield of 2-(*o*-tolylloxy)ethan-1-ol (**bf**) 1-(4-methoxyphenyl)-2-methoxyphenyl-2-phenoxypropane-1,3-diol (**J**); 78% yield of **aa** and 70% yield of 2-(2-methoxyphenoxy)ethan-1-ol (**bg**) for 2-(2-methoxyphenoxy)-1-(4-methoxyphenyl)propane-1,3-diol (**K**) (Table 2, entries 8 to 11). These results indicated that the PCET strategy exhibited high selectivity towards  $\beta$ -scission occurred at  $\text{C}_\alpha\text{-C}_\beta$  bond, leaving  $\text{C}_\beta\text{-C}_\gamma$  and  $\text{C-O}$  bonds intact. It should be noted that a 100 W blue LED lamp is required to obtain good to high product yield for reaction using lignin model **F**, **G** or **K** with potential less than 1.05 V ( $E_{\text{p}/2} = 1.05 \text{ V}$  for **F**, 1.05 V for **G** and 1.02 V for **K**, vs.  $\text{Fc/Fc}^+$ ) as substrate. However, poor catalytic performance was observed for collidine-based PCET reactions using lignin model with an even lower redox potential ( $E_{\text{p}/2} = 0.94 \text{ V}$  for **L**, 0.85 V for **M**, 0.87 V for **N**, 0.85 V for **O** vs.  $\text{Fc/Fc}^+$ ) as substrates, including *G*-/*S*-lignin models 1-(3,4-dimethoxyphenyl)-2-phenoxypropane-1,3-diol (**L**), 1-(3,4-dimethoxyphenyl)-2-(2-methoxyphenoxy)propane-1,3-diol (**M**), 2-(2-methoxyphenoxy)-1-(3,4,5-trimethoxyphenyl)propane-1,3-diol (**N**) and 2-(2-methoxyphenoxy)-1-(3,4,5-trimethoxyphenyl)propane-1,3-diol (**O**). For example, lignin model **M**/collidine PCET pair possessing a low BDFE value of 95 kcal/mol only obtained 3,4-dimethoxybenzaldehyde (**ae**) and **bg** in 25% yield, respectively (Table S1 online, entry 1), indicating that we might need to explore a base with higher alkalinity to bring up the BDFE value close to 102 kcal/mol so that PCET reaction is feasible. To this context, a strong base  $\text{NBu}_4\text{OBz}$  ( $\text{pK}_a = 21.5$ ) was combined with model **M** to form a PCET pair with a BDFE of 104 kcal/mol, only less than 8% product yield was obtained for PCET reaction performed in  $\text{CH}_2\text{Cl}_2$  (Table S1 online, entry 2). Therefore, we examined the effectiveness of different reaction parameters on PCET reaction. Such as the employment of  $\text{CH}_3\text{CN}$  as solvent enabled us to achieve a drastically enhanced yield of **ae** (74%) and **bg** (71%) (Table S1 online, entry 3) whereas an increase in the power of blue LED lamp from 50 to 100 W led to



**Table 2**

Selective C $_{\alpha}$ –C $_{\beta}$  bond cleavage in different lignin models by photocatalytic depolymerization strategy.<sup>a</sup>



Entry	Substrate ( $E_{p/2}$ , vs. Fc/Fc <sup>+</sup> )	Conv. (%) <sup>b</sup>	Yield (%) <sup>b</sup>
1	<b>A</b> (1.16 V)	>99	<b>aa</b> , 94 (92) <b>ba</b> , 93 (90)
2	<b>B</b> (1.21 V)	>99	<b>ab</b> , 95 (90) <b>ba</b> , 93 (91)
3	<b>C</b> (1.24 V)	>99	<b>ac</b> , 92 (85) <b>ba</b> , 91 (83)
4	<b>D</b> (1.24 V)	>99	<b>ad</b> , 95 (94) <b>ba</b> , 92 (89)
5	<b>E</b> (1.17 V)	>99	<b>aa</b> , 95 (89) <b>bb</b> , 96 (90)
6 <sup>c</sup>	<b>F</b> (1.05 V)	>99	<b>aa</b> , 94 (86) <b>bc</b> , 93 (84)
7 <sup>c</sup>	<b>G</b> (1.05 V)	>99	<b>aa</b> , 89 (85) <b>bd</b> , 86 (80)
8	<b>H</b> (1.26 V)	85	<b>ab</b> , 80 (74) <b>be</b> , 78 (69)
9	<b>I</b> (1.11 V)	>99	<b>aa</b> , 97 (95) <b>be</b> , 90 (88)
10	<b>J</b> (1.12 V)	>99	<b>aa</b> , 94 (85) <b>bf</b> , 91 (80)
11 <sup>c</sup>	<b>K</b> (1.02 V)	82	<b>aa</b> , 78 (67) <b>bg</b> , 70 (61)
12 <sup>c,d</sup>	<b>L</b> (0.94 V)	93	<b>ae</b> , 82 (75) <b>be</b> , 71 (64)
13 <sup>c,d</sup>	<b>M</b> (0.85 V)	96	<b>ae</b> , 91 (89) <b>bg</b> , 83 (80)
14 <sup>c,d</sup>	<b>N</b> (0.87 V)	86	<b>af</b> , 80 (74) <b>be</b> , 72 (68)
15 <sup>c,d</sup>	<b>O</b> (0.85 V)	87	<b>af</b> , 80 (72) <b>bg</b> , 71 (58)
16	<b>P</b> (1.08 V)	>99	<b>aa</b> , 96 (92) <b>bh</b> , 94 (65)

<sup>a</sup> Reaction were performed with 0.1 mmol substrate, 2 mol% **Ir-1**, 20 mol% collidine, 10 mol% PhSH in 2 mL CH<sub>2</sub>Cl<sub>2</sub> and illuminated with 50 W blue LED lamp in N<sub>2</sub> atmosphere at RT for 12 h.

<sup>b</sup> Conversion and yield were measured by HPLC. Isolated product yield in parenthesis.

<sup>c</sup> Illuminated with 100 W blue LED lamp.

<sup>d</sup> After the first batch of reaction mixture containing 0.1 mmol substrate, 1 mol% **Ir-1**, 10 mol% NBu<sub>4</sub>OBz, 5 mol% PhSH and 2 mL CH<sub>3</sub>CN illuminated by 100 W blue LED lamp at RT for 6 h, the second batch of catalytic mixtures including 1 mol% **Ir-1**, 10 mol% NBu<sub>4</sub>OBz and 5 mol% PhSH was added and illuminated for another 6 h.

nin models **L** and S-type lignin models **N** and **O** as substrate through the same procedure (Table 2, entries 12, 14, and 15).

It is known that C–C bond cleavage of  $\beta$ -1 model is more efficient than that of  $\beta$ -O-4 model [55]. Many advancements have been achieved in the selective C–C bond cleavage of  $\beta$ -1 models [25,56,57]. Success achieved in the selective C $_{\alpha}$ –C $_{\beta}$  bond cleavage in  $\beta$ -O-4 lignin models promoted us to apply this facile visible-light driven photocatalytic strategy to the degradation of  $\beta$ -1 lignin model, 1-(4-methoxyphenyl)-2-phenylethan-1-ol (**P**) with a  $\alpha$ -OH group. Since the redox potential of model **P** ( $E_{p/2}$  = 1.08 V vs. Fc/Fc<sup>+</sup>) is similar to that of model **A**, therefore, a model **P**/collidine PCET pair was employed to achieve a 96% yield of **aa** and 94% yield of toluene (**bh**) (Table 2, entry 16). These results further highlighted the importance of considering both alkalinity of the base and redox potential of the lignin model substrate when matching base with lignin model substrate for generating a suitable PCET pair [37].

### 3.3. Mechanistic studies

Previously, Knowles and co-workers [42] proposed that the generation of alkoxy radical intermediates via multisite PCET activation of alcohol O–H bonds is essentially important to the catalytic ring-opening of cyclic alcohols into linear ketone product, since it could substantially weaken adjacent C–C bonds. Different from cyclic alcohols reported in their studies, we investigate PCET reaction using linear lignin model compounds as substrates. The combination of experimental details and mechanism previously reported in literatures [42,58–61] led to a possible reaction mechanism for C $_{\alpha}$ –C $_{\beta}$  bond cleavage in  $\beta$ -O-4 lignin model via PCET process (Fig. 2). In which, **Ir**<sup>III</sup> containing compound (**Ir**<sup>III</sup>) was excited to **\*Ir**<sup>III</sup> containing compound (**\*Ir**<sup>III</sup>) under the illumination of blue light. In the presence of a base, intermolecular hydrogen bond was formed with lignin model [58–61], and then electron was transferred from the phenyl moiety (adjacent to  $\alpha$ -OH group, red) of lignin model to **\*Ir**<sup>III</sup> to produce an **Ir**<sup>II</sup> containing compound (**Ir**<sup>II</sup>) along with the generation of a radical cationic intermediate, which went through PCET process to furnish an alkoxy radical intermediate. This alkoxy radical will weaken the neighboring C $_{\alpha}$ –C $_{\beta}$  bond, thus achieving the  $\beta$ -scission of C $_{\alpha}$ –C $_{\beta}$  bond to produce benzaldehyde and carbon free-radical, which could be trapped by hydrogen atom transfer (HAT) of thiophenol to form anisole along with the production of PhS $\cdot$  radical. Oxidization of **Ir**<sup>II</sup> by PhS $\cdot$  radical will regenerate both **Ir**<sup>III</sup> and PhSH for the next catalytic cycle. Processes of electron transfer (ET), PCET, and  $\beta$ -scission shown in the mechanism were similar with that previously proposed by Knowles and co-workers [42] based on the Stern-Volmer analysis and DFT calculation. Except that, we found the following evidences to provide further support for the proposed mechanism: (i) the fact that unsuccessful PCET reaction by **Ir-2** with redox potential lower than that of the model substrate provides further evidence to support the photoinduced ET process (Table 1, entry 13). (ii) Adding TEMPO to reaction led to a drastically decreased conversion of lignin model (7%), which also confirmed that the photocatalytic reaction is initiated by a free radical (Scheme S2 online). (iii) Also noted that there are multiple hydrogen transfers (PCET, HAT and PT) involved in the reaction as shown in the mechanism, which could be verified by isotope-labelling experiments performed with deuterated  $\alpha$ -OH of lignin model **A** (**d**<sub>1</sub>-**A**) as substrate (Fig. S1 online). As revealed by <sup>1</sup>H NMR spectra, selective cleavage of C $_{\alpha}$ –C $_{\beta}$  bond in **d**<sub>1</sub>-**A** afforded **aa** and **ba** under the excitation of blue light while a set of triplets observed at 3.8 ppm might be attributed to **d**<sub>1</sub>-anisole (PhOCH<sub>2</sub>D). GC/MS measurement further confirmed the formation of **d**<sub>1</sub>-anisole (109.21 *m/z*, Fig. S2 online). These results are consistent with the proposed mechanism as shown in Fig. 2.

the further enhancement of product yield (83% **ae**; 74% **bg**, Table S1 online, entry 4). Interestingly, the product yield of **ae** and **bg** could be further enhanced to 91% and 83%, respectively (Table 2, entry 13), when we divided the catalytic mixture of **Ir-1**, NBu<sub>4</sub>OBz and PhSH into two portions and added the first one in the beginning of the reaction and the second one after 6 h of reaction. Good to high product yield could be achieved by reactions using G-type lig-

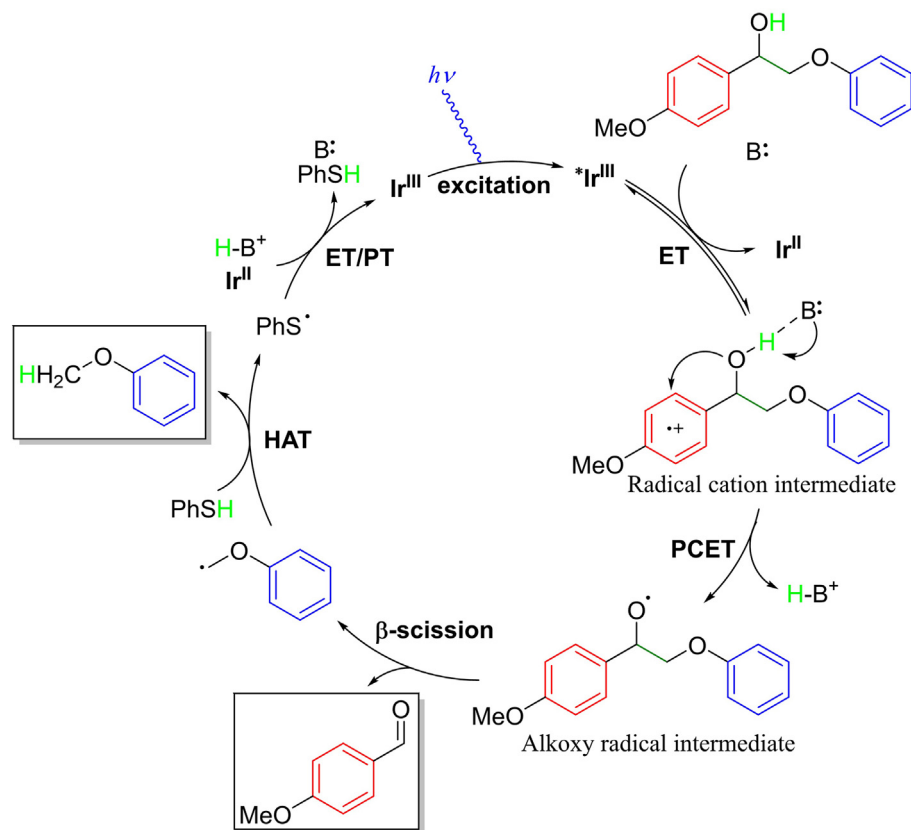
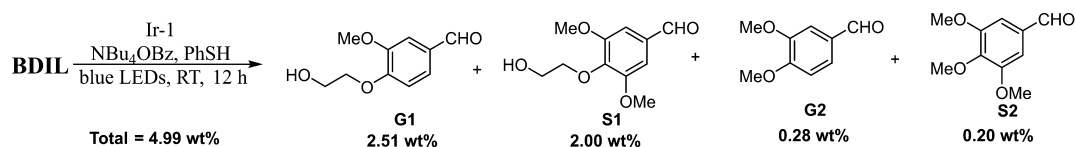


Fig. 2. (Color online) Plausible mechanism for selective C<sub>α</sub>-C<sub>β</sub> bond cleavage by Ir-1 via PCET process.



Scheme 2. Selective C<sub>α</sub>-C<sub>β</sub> bond cleavage of BDIL.

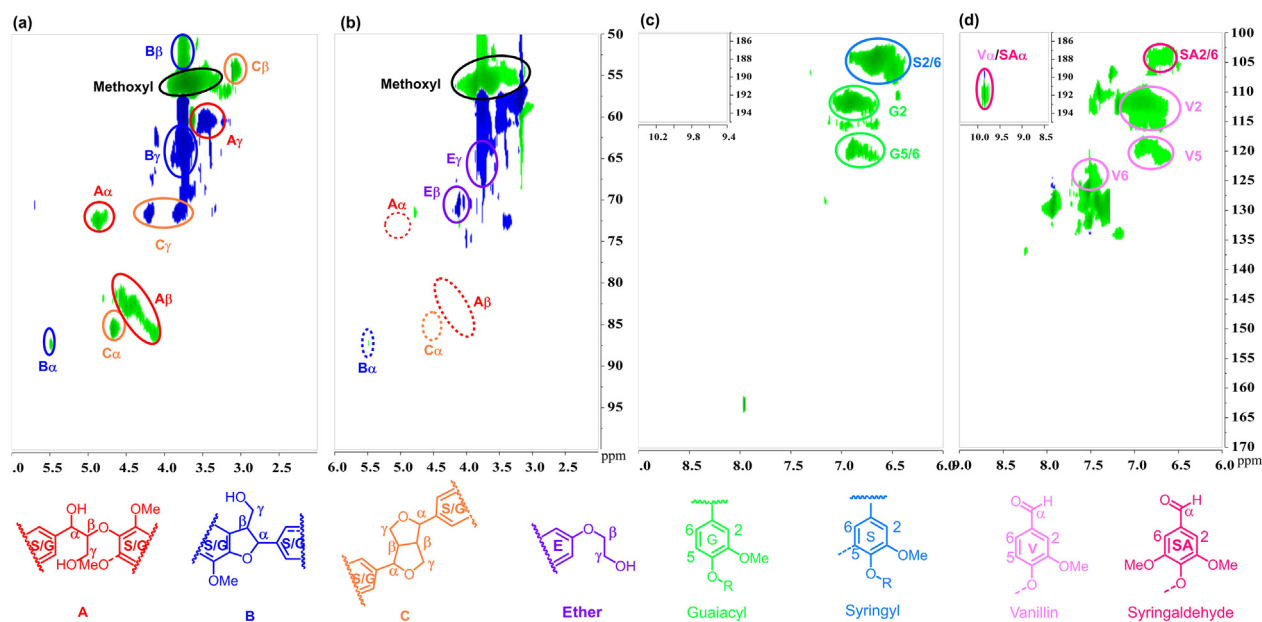


Fig. 3. (Color online) 2D HSQC spectra of BDIL in d-DMSO. (a), (c) BDIL before depolymerization; (b), (d) BDIL after depolymerization.

Furthermore, since the formation of a phenyl radical cation is essentially important for the subsequent PCET reaction according to the mechanism, the presence of strong electron-donating, such as methoxy group, on phenyl ring (left, red) is considered to be beneficial for the generation of phenyl radical cation intermediate due to its capability of stabilizing the radical cation, and vice versa [62]. However, contrary to the expected, high to near quantitative conversion and good yield of C–C bond cleavage product could still be achieved by lignin models **B**, **C** and **H** without -OMe group on the left phenyl ring. It might be attributed to the presence of right phenoxy group in lignin model **B**, **C** and **H**, which is prone to be oxidized into radical cation intermediate, thus enabling the C $_{\alpha}$ –C $_{\beta}$  bond cleavage via longer distance PCET reaction. Such speculation could be confirmed by control experiment that using 1,2-diphenyl-1-ethanol without methoxy group (left) and phenoxy group (right) as substrate completely quenched PCET reaction (Scheme S3 online).

### 3.4. The degradation of lignin

To investigate the practical application of this PCET method, we have examined various reaction parameters of this Ir-based photocatalytic system for the degradation of **BDL** prepared through extraction of birch lignin with HCl/dioxane, but did not obtain any positive results. Moreover, we observed low catalytic performance for PCET reaction using lignin substrate with hydroxyl group on phenoxy ring (Scheme S4 online). Therefore, we employed MeI/K $_2$ CO $_3$  to selectively protect the possible phenolic hydroxyl groups on phenoxy ring of **BDL** to produce a **BDIL**. Depolymerization of **BDIL** by PCET method led to an enhanced degradation product yield of 4.99 wt% (Scheme 2, Fig. S3 online). GPC traces provide evidences to further support the successful depolymerization of **BDIL**, showing an obvious shift to a smaller-molecular weight region for degradation product in comparison with that for corresponding lignin before depolymerization (Fig. S4 online).

The analysis of 2D HSQC results revealed that the major peaks attributed to  $\beta$ -O-4 units (A) had completely disappeared after depolymerization of **BDIL** and new cross peaks are consistent with the expected cleavage product (Fig. 3). More specifically, the selective cleavage of C $_{\alpha}$ –C $_{\beta}$  bond led to the disappearance of A $_{\alpha}$  ( $\delta_C$  73,  $\delta_H$  5.0 ppm) and A $_{\beta}$  ( $\delta_C$  84,  $\delta_H$  4.2 ppm) in  $\beta$ -O-4 as well as the formation of corresponding aldehyde group V $\alpha$  and SA $_{\alpha}$  ( $\delta_C$  192,  $\delta_H$  9.8 ppm) attributed to ether product (E) (E $_{\beta}$  ( $\delta_C$  70,  $\delta_H$  4.1 ppm) and E $_{\gamma}$  ( $\delta_C$  65,  $\delta_H$  3.6 ppm)). Furthermore, analysis of the aromatic regions (Fig. 3c and d) indicated that the majority of G-type lignin (G) (G2 ( $\delta_C$  112,  $\delta_H$  6.9 ppm), G5/G6 ( $\delta_C$  119,  $\delta_H$  6.8 ppm)) and S-type lignin (S) (S2/6 ( $\delta_C$  104,  $\delta_H$  6.7 ppm)) found in **BDIL** were converted to aromatic ring (V2 ( $\delta_C$  112,  $\delta_H$  6.9 ppm), V5 ( $\delta_C$  120,  $\delta_H$  7.0 ppm) and V6 ( $\delta_C$  125,  $\delta_H$  7.5 ppm)) attributed to unit V and SA2/6 ( $\delta_C$  103,  $\delta_H$  7.0 ppm) to unit SA. These results demonstrate the high effectivity and selectivity of this redox-neutral PCET strategy at RT towards the C $_{\alpha}$ –C $_{\beta}$  bond scission in real lignin depolymerization.

## 4. Conclusion

In conclusion, we have developed a one-step, visible-light-driven photocatalytic strategy for selective C $_{\alpha}$ –C $_{\beta}$  bond cleavage in lignin models via multisite PCET activation of  $\alpha$ -OH bond at RT, by choosing suitable combination of a base with appropriate alkalinity (pK $_a$ ) and different lignin model substrates with a BDFE close to the BDE of O–H bond (102 kcal/mol). This method enable us to successfully take full advantage of the structural characteris-

tic of lignin model substrates including  $\beta$ -O-4 and  $\beta$ -1 linkages, which not only circumvent the pretreatment of  $\alpha$ -OH that requires extra energy cost and multisteps, but also achieve corresponding C $_{\alpha}$ –C $_{\beta}$  bond cleavage products in high to excellent yields and selectivities, such as aromatic aldehydes (up to 97% yield) and phenol ethers or toluene (up to 96% yield). It is a truly 100% atom economic, redox-neutral depolymerization strategy without the breakdown of C $_{\beta}$ –C $_{\gamma}$  or C $_{\beta}$ –O bonds or loss of any atom. More importantly, this PCET method is demonstrated to be effective for the depolymerization of real lignin at RT. These results will provide significantly important foundation to the valorisation of lignin in the future.

## Conflict of interest

The authors declare that they have no conflict of interest.

## Acknowledgments

This work was supported by the National Natural Science Foundation of China (21975102, 21871107, 21774042, and 21422401).

## Author contributions

Yuetao Zhang acquired the fund, conceived the project and directed research. Yinling Wang designed and conducted experiments. Yue Liu synthesized the catalysts. Yinling Wang, Jianghua He and Yuetao Zhang analyzed the data and wrote the manuscript.

## Appendix A. Supplementary materials

Supplementary materials to this article can be found online at <https://doi.org/10.1016/j.scib.2019.09.003>.

## References

- [1] Boerjan W, Ralph J, Baucher M. Lignin biosynthesis. *Annu Rev Plant Biol* 2003;54:519–46.
- [2] Fan H, Yang Y, Song J, et al. One-pot sequential oxidation and aldolcondensation reactions of veratryl alcohol catalyzed by the Ru@ZIF-8 + CuO/basic ionic liquid system. *Green Chem* 2014;16:600–4.
- [3] Corma A, Iborra S, Velty A. Chemical routes for the transformation of biomass into chemicals. *Chem Rev* 2007;107:2411–502.
- [4] Li C, Zhao X, Wang A, et al. Catalytic transformation of lignin for the production of chemicals and fuels. *Chem Rev* 2015;115:11559–624.
- [5] Sanderson K. A Chewy problem. *Nature* 2011;474:S12–4.
- [6] Son S, Toste FD. Non-oxidative vanadium-catalyzed C–O bond cleavage: application to degradation of lignin model compounds. *Angew Chem Int Ed* 2010;49:3791–4.
- [7] Sergeev AG, Hartwig JF. Selective, nickel-catalyzed hydrogenolysis of aryl ethers. *Science* 2011;332:439–43.
- [8] Gao F, Webb JD, Hartwig JF. Chemo- and regioselective hydrogenolysis of diaryl ether C–O bonds by a robust heterogeneous Ni/C catalyst: applications to the cleavage of complex lignin-related fragments. *Angew Chem* 2016;55:1474–8.
- [9] Nguyen JD, Matsuura BS, Stephenson CR. A photochemical strategy for lignin degradation at room temperature. *J Am Chem Soc* 2014;136:1218–21.
- [10] Nichols JM, Bishop LM, Bergman RG, et al. Catalytic C–O bond cleavage of 2-aryloxy-1-arylethanol and its application to the depolymerization of lignin-related polymers. *J Am Chem Soc* 2010;132:12554–5.
- [11] Rahimi A, Ulbrich A, Coon JJ, et al. Formic-acid-induced depolymerization of oxidized lignin to aromatics. *Nature* 2014;515:249–52.
- [12] Shuai L, Amiri MT, Questell-Santiago YM, et al. Formaldehyde stabilization facilitates lignin monomer production during biomass depolymerization. *Science* 2016;354:329–33.
- [13] Lahive CW, Deuss PJ, Lancefield CS, et al. Advanced model compounds for understanding acid-catalyzed lignin depolymerization: identification of renewable aromatics and a lignin-derived solvent. *J Am Chem Soc* 2016;138:8900–11.
- [14] Feghali E, Carrot G, Thuéry P, et al. Convergent reductive depolymerization of wood lignin to isolated phenol derivatives by metal-free catalytic hydrosilylation. *Energy Environ Sci* 2015;8:2734–43.

- [15] Zhang J, Li Y, Xu R, et al. Donor-acceptor complex enables alkoxyl radical generation for metal-free C(sp<sup>3</sup>)-C(sp<sup>3</sup>) cleavage and allylation/alkenylation. *Angew Chem Int Ed* 2017;56:12619–23.
- [16] Jia K, Zhang F, Huang H, et al. Visible-light-induced alkoxyl radical generation enables selective C(sp<sup>3</sup>)-C(sp<sup>3</sup>) bond cleavage and functionalizations. *J Am Chem Soc* 2016;138:1514–7.
- [17] Zhu J, Wang J, Dong G. Catalytic activation of unstrained C(aryl)-C(aryl) bonds in 2,2'-biphenols. *Nat Chem* 2019;11:45–51.
- [18] vom Stein T, den Hartog T, Buendia J, et al. Ruthenium-catalyzed C–C bond cleavage in lignin model substrates. *Angew Chem Int Ed* 2015;54:5859–63.
- [19] Lancefield CS, Teunissen LW, Weckhuysen BM, et al. Iridium-catalysed primary alcohol oxidation and hydrogen shuttling for the depolymerisation of lignin. *Green Chem* 2018;20:3214–21.
- [20] Luo N, Wang M, Li H, et al. Visible-light-driven self-hydrogen transfer hydrogenolysis of lignin models and extracts into phenolic products. *ACS Catal* 2017;7:4571–80.
- [21] Luo N, Wang M, Li H, et al. Photocatalytic oxidation-hydrogenolysis of lignin β-O-4 models via a dual light wavelength switching strategy. *ACS Catal* 2016;6:7716–21.
- [22] Wu X, Chen L, Fan X, et al. Solar energy-driven lignin-first approach to full utilization of lignocellulosic biomass under mild conditions. *Nat Catal* 2018;1:772–80.
- [23] Luo J, Zhang X, Lu J, et al. Fine tuning the redox potentials of carbazolic porous organic frameworks for visible-light photoredox catalytic degradation of lignin β-O-4 models. *ACS Catal* 2017;7:5062–70.
- [24] Liu H, Li H, Lu J, et al. Photocatalytic cleavage of C–C bond in lignin models under visible light on mesoporous graphitic carbon nitride through π-π stacking interaction. *ACS Catal* 2018;8:4761–71.
- [25] Hou T, Luo N, Li H, et al. Yin and Yang dual characters of Cu<sub>2</sub>O<sub>2</sub> clusters for C–C bond oxidation driven by visible light. *ACS Catal* 2017;7:3850–9.
- [26] Wang M, Lu J, Zhang X, et al. Two-step, catalytic C–C bond oxidative cleavage process converts lignin models and extracts to aromatic acids. *ACS Catal* 2016;6:6086–90.
- [27] Dabral S, Hernández JG, Kamer PCJ, et al. Organocatalytic chemoselective primary alcohol oxidation and subsequent cleavage of lignin model compounds and lignin. *ChemSusChem* 2017;10:2707–13.
- [28] Wang Y, Wang Q, He J, et al. Highly effective C–C bond cleavage of lignin model compounds. *Green Chem* 2017;19:3135–41.
- [29] Wang Y, Du Y, He J, et al. Transformation of lignin model compounds to N-substituted aromatics via beckmann rearrangement. *Green Chem* 2018;20:3318–26.
- [30] Rahimi A, Azarpira A, Kim H, et al. Chemoselective metal-free aerobic alcohol oxidation in lignin. *J Am Chem Soc* 2013;135:6415–8.
- [31] Parthasarathi R, Romero RA, Redondo A, et al. Theoretical study of the remarkably diverse linkages in lignin. *J Phys Chem Lett* 2011;2:2660–6.
- [32] Kim S, Chmely SC, Nimlos MR, et al. Computational study of bond dissociation enthalpies for a large range of native and modified lignins. *J Phys Chem Lett* 2011;2:2846–52.
- [33] Lancefield CS, Ojo OS, Tran F, et al. Isolation of functionalized phenolic monomers through selective oxidation and C–O bond cleavage of the β-O-4 linkages in lignin. *Angew Chem Int Ed* 2015;54:258–62.
- [34] Zhu R, Wang B, Cui M, et al. Chemoselective oxidant-free dehydrogenation of alcohols in lignin using Cp\*Ir catalysts. *Green Chem* 2016;18:2029–36.
- [35] Huynh MHV, Meyer TJ. Proton-coupled electron transfer. *Chem Rev* 2007;107:5004–64.
- [36] Warren JJ, Tronic TA, Mayer JM. Thermochemistry of proton-coupled electron transfer reagents and its implications. *Chem Rev* 2010;110:6961–7001.
- [37] Waidmann CR, Miller AJM, Ng C-WA, et al. Using combinations of oxidants and bases as PCET Reactants: thermochemical and practical considerations. *Energy Environ Sci* 2012;5:7771–80.
- [38] Choi GJ, Knowles RR. Catalytic alkene carboaminations enabled by oxidative proton-coupled electron transfer. *J Am Chem Soc* 2015;137:9226–9.
- [39] Miller DC, Choi GJ, Orbe HS, et al. Catalytic olefin hydroamidation enabled by proton-coupled electron transfer. *J Am Chem Soc* 2015;137:13492–5.
- [40] Choi GJ, Zhu Q, Miller DC, et al. Catalytic alkylation of remote C–H bonds enabled by proton-coupled electron transfer. *Nature* 2016;539:268–71.
- [41] Zhu Q, Graff DE, Knowles RR. Intermolecular anti-markovnikov hydroamination of unactivated alkenes with sulfonamides enabled by proton-coupled electron transfer. *J Am Chem Soc* 2018;140:741–7.
- [42] Yayla HG, Wang H, Tarantino KT, et al. Catalytic ring-opening of cyclic alcohols enabled by PCET activation of strong O–H bonds. *J Am Chem Soc* 2016;138:10794–7.
- [43] Schultz DM, Yoon TP. Solar synthesis: prospects in visible light photocatalysis. *Science* 2014;343:1239176.
- [44] Lang X, Chen X, Zhao J. Heterogeneous visible light photocatalysis for selective organic transformations. *Chem Soc Rev* 2014;43:473–86.
- [45] Zhang T, Lin W. Metal-organic frameworks for artificial photosynthesis and photocatalysis. *Chem Soc Rev* 2014;43:5982–93.
- [46] Twilton J, Le CC, Zhang P, et al. The merger of transition metal and photocatalysis. *Nat Rev Chem* 2017;1:0052.
- [47] Ota E, Wang H, Frye NL, et al. A redox strategy for light-driven, out-of-equilibrium isomerizations and application to catalytic C–C bond cleavage reactions. *J Am Chem Soc* 2019;141:1457–62.
- [48] Colombo MG, Hauser A, Giidel HU. Evidence for strong mixing between the LC and MLCT excited states in bis(2-phenylpyridinato-C<sup>2</sup>,N')(2,2'-bipyridine) iridium(III). *Inorg Chem* 1993;32:3088–92.
- [49] Sun Y, Giebink NC, Kanno H, et al. Management of singlet and triplet excitons for efficient white organic light-emitting devices. *Nature* 2006;440:908–12.
- [50] Gärtner F, Sundararaju B, Surkus A-E, et al. Eisencarbonyl: effiziente katalysatoren für die lichtgetriebene wasserstoffzeugung aus wasser. *Angew Chem* 2009;121:10147–50.
- [51] Hoffmann N. Proton-coupled electron transfer in photoredox catalytic reactions. *Eur J Org Chem* 2017;15:1982–92.
- [52] Baranoff E, Yum JH, Jung I, et al. Cyclometallated iridium complexes as sensitizers for dye-sensitized solar cells. *Chem Asian J* 2010;5:496–9.
- [53] Kaljurand I, Agnes Kütt LS, Rodima T, et al. Extension of the self-consistent spectrophotometric basicity scale in acetonitrile to a full span of 28 pK<sub>a</sub> units: unification of different basicity scales. *J Org Chem* 2005;70:1019–28.
- [54] Luo Y-R. Handbook of bond dissociation energies in organic compounds. Boca Raton: CRC Press; 2003.
- [55] Cho DW, Parthasarathi R, Pimentel AS, et al. Nature and kinetic analysis of carbon-carbon bond fragmentation reactions of cation radicals derived from SET-oxidation of lignin model compounds. *J Org Chem* 2010;75:6549–62.
- [56] Zhou Z, Liu M, Li C-J. Selective copper-N-heterocyclic carbene (copper-NHC)-catalyzed aerobic cleavage of β-1 lignin models to aldehydes. *ACS Catal* 2017;7:3344–8.
- [57] Sedai B, Díaz-Urrutia C, Baker RT, et al. Aerobic oxidation of β-1 lignin model compounds with copper and oxovanadium catalysts. *ACS Catal* 2013;3:3111–22.
- [58] Baciocchi E, Bietti M, Putignani L, et al. Side-chain fragmentation of arylalkanol radical cations. Carbon-carbon and carbon-hydrogen bond cleavage and the role of α- and β-OH groups. *J Am Chem Soc* 1996;118:5952–60.
- [59] Baciocchi E, Bietti M, Steenken S. Base-catalyzed C–H deprotonation of 4-methoxybenzyl alcohol radical cations in water: evidence for a carbon-to-oxygen 1,2-H-shift mechanism. *J Am Chem Soc* 1997;119:4078–9.
- [60] Baciocchi E, Bietti M, Lanzalunga O, et al. Oxygen acidity of 1-arylalkanol radical cations. 4-Methoxycumyloxy radical as -C(Me)<sub>2</sub>-O<sup>•</sup> to-nucleus electron-transfer intermediate in the reaction of 4-methoxycumyl alcohol radical cation with OH<sup>•</sup>. *J Am Chem Soc* 1998;120:11516–7.
- [61] Baciocchi E, Bietti M, Lanzalunga O. Mechanistic aspects of β-Bond-cleavage reactions of aromatic radical cations. *Acc Chem Res* 2000;33:243–51.
- [62] Jonsson M, Lind J, Reitberger T, et al. Redox chemistry of substituted benzenes: the one-electron reduction potentials of methoxy-substituted benzene radical cations. *J Phys Chem* 1993;97:11278–82.



Yinling Wang obtained her Ph.D. degree under the supervision of Prof. Yuetao Zhang from Department of Organic Chemistry, Jilin University in 2019. Her research interests are focused on the field of photocatalytic chemistry and biomass degradation.



Jianghua He received her B.S. degree from Changchun Normal University in 1999, M.S. degree supervised by Prof. Jingfu Liu at the Northeast Normal University in 2002 and Ph.D. degree under the direction of Prof. Jihong Yu from the State Key Laboratory of Inorganic Synthesis & Preparative Chemistry, Jilin University in 2005. She served as a postdoctoral research fellow at Prof. Bruce Parkinson's lab from 2007 to 2009 and in Eugene Y.-X. Chen's lab at Colorado State University since 2011, where she was promoted as Research Scientist I in 2013. She moved to Jilin University as associate professor at the College of Chemistry, Jilin University in 2015. Her research interests are focused on the polymer synthesis and biomass conversion.





Yuetao Zhang received his B.S. degree from Jilin University in 1999 and Ph.D. degree under the Prof. Ying Mu's direction from Department of Organic Chemistry, Jilin University in 2004. He joined the Prof. Eugene Y.-X. Chen's lab at Colorado State University as a postdoctoral research fellow in 2006 and promoted as Research Scientist III in 2009. He moved to Jilin University as a full professor at the State Key Laboratory of Supramolecular Structure and Materials of College of Chemistry in 2013 and was awarded the "NSFC Excellent Young Scholar Fellowship" in 2014. His current research interests span broadly the areas of polymer science, organic synthetic

chemistry, catalytic chemistry as well as green and sustainable chemistry, such as the design and synthesis of living/controlled catalyst system for polar vinyl monomers and cyclic esters; synthesis of sustainable polymers from renewable feedstocks; production of platform chemicals, energy and fuels from biomass conversion.